

Analysing Banding Features for Classifying Print Processes using Artificial Neural Networks

Shankhya Debnath and Jitamitra Bagchi; Department of Printing Engineering, Jadavpur University, Kolkata, India

Abstract

The need for verifying and authenticating printed documents for the purpose of determining its validity finds applications in various fields, including digital forensic analysis and forgery detection. Print security becomes a primary concern for end use consumers and application providers at all levels of usage. Identifying the authenticity of a print can be a challenging task, since print quality and features varies on varying the methods of printing. In order to determine the source or process of printing, various methods has been specified in literature. This paper provides an in depth analysis on one such measure. Each printer has some features which are inherently part of the process due to the mechanical parameters used while modelling the device. Such features may be called intrinsic features of a printer. One of these primary features is banding that occurs primarily in electrophotographic(EP) printing processes, which has been widely reported in standard literature. However, such existence in offset or gravure printing is yet to be verified. This paper deals with examining the presence of such banding frequencies in offset or gravure printing processes. Numbers of printing processes were examined and thereby the banding was analysed using their corresponding frequency spectrum. The data obtained from the method were used as features for classifying the printing method using a supervised multilevel perceptron.

Introduction

It becomes very important for securing different forms in order to protect the copyright and verifying its authenticity [1, 2]. Identification of printer for forensic analysis deals with extracting certain properties which are inherent to a printer of a particular make and model which distinguishes it from other manufacturers. Such features can be called intrinsic features of the printer [3]. Analysis of such features needs realization of the concepts and mechanism of a particular printer and how it works. One such feature which is predominant in most electrophotographic printers is occurrence of banding throughout the length of the printed page. [4-10] have shown in their works the methods that make use of these banding frequencies for identifying a printer.

There are primarily two aspects for analysing the banding in printing processes. One being the human visualization of this banding and creating a threshold for reaching an acceptable criterion. The other being the analysis of these banding structures for the purpose of associating print processes with the various machines, which uses a frequency domain analysis of projected images [11]. The banding frequency is dominantly visible in midtone areas and along the direction of processing of the paper. These features are not always visible to the human eyes, but can be

detected by appropriate algorithms. Analysis of the Fourier Transform(DFT) and the Power Spectrum from the horizontally projected images has been used for depicting banding and segregating it from graininess and other print problems [12, 13, 14, 15]. The variations of banding frequency with other printer parts have also been studied [16, 17, 18, 19]. Human visual perception of banding and its reduction by thresholding techniques have been studied in [20, 21, 22, 23].

A predominant problem that occurs in the EP process is quasiperiodic fluctuations in the printing processes, which causes banding [4]. They are mainly caused by the fluctuations in the angular velocity of the photoconductor cylinder, leading to creation of horizontal lines which are not uniform. This in turn leads to fluctuations in the toner distributions of the printed image [24]. The banding phenomenon is related to gear movement of the printer and hence can be viewed as a direct consequence of the mechanical modelling of the printer. However, the existence of banding in offset or gravure processes is yet to be seen. The process of printing in both gravure and offset is much similar to EP printing. Since all of them are direct transfer based printing. The substrate is made to pass through two cylinder construction. There is a possibility of quasiperiodic fluctuations occurring since these cylinders are not continuous but have a break along there surface for inserting plates.

This paper is divided into four parts. The introductory stage gives a brief idea about the background of the study and focuses on the literature survey executed prior to the work. The second part describes the experimental methodology and the structure of work done. The discussions are comprised in the third section which deals with the results of the experiment and finally the scope of improvement and further remarks are cited in the conclusion section.

Experimental Design

In order to use the banding frequencies as a feature for classifying printing methods, the following design was adopted. Various prints from different printing methods were adopted, which included laser, offset and gravure. These prints were then used for feature extraction. This work mainly deals with analysing and extracting banding features that occurs due to printer shortcomings. These images were then scanned with the help of a moderately powered HP Deskjet 1050 multipurpose scanner at a resolution of 1200 dpi, which rendered satisfactory digital images. There were a total of 90 prints that were used for scanning, each of these prints contained a variety of matter including both text and image regions, however average key images were primarily chosen as it has been stated above that the banding structure becomes predominant mainly in the midtone areas.

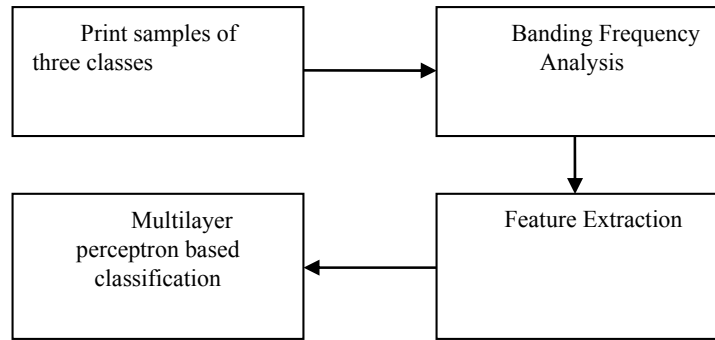


Figure 1: Schematic for experimental process

Once these images were obtained, they were processed using image processing software. In order to reduce complexity of operations, the digital images were converted into their corresponding grayscale images. During the conversion, any degradation of quality was avoided except for the loss of color values, and hence the images maintained their original resolution while being processed. This was followed by projecting each image $I(x,y)$ horizontally to produce $\text{proj}(x)=\sum_y I(x,y)$ as has been shown in Figure 3. Once these plots were available, then a fourier analysis of these curves were computed to obtain the Figure 4. From these plots the spikes were analysed and used as features for the classifier.

The need for conversion of time series data into the frequency domain, comes from the fact that all these images that are to be analysed contains periodic noise embedded into the time signal. However it is not possible to analyse these periodicities unless the discrete signal is sampled in the frequency domain. This conversion can be achieved by means of using a forward fourier transform or simply a fourier transform. The Fourier transform is a representation of an image as a sum of complex exponentials of varying magnitudes, frequencies, and phases. Since the images taken were all sampled at a specific level, a discrete fourier transform had to be used for the purpose. However, a faster implementation for the same algorithm is known as a fast fourier transform which gives a similar result. The discrete fourier transform (DFT) is usually defined for a discrete function $f(m,n)$ that is non zero only over the finite region $0 \leq m \leq M-1$ and $0 \leq n \leq N-1$. Two dimensional M-by-N DFT is given by,

$$F(p, q) = \sum_{m=0}^{M-1} \sum_{n=0}^{N-1} f(m, n) e^{-\frac{j2\pi pm}{M}} e^{-\frac{j2\pi qn}{N}} \quad \text{for } p=0,1,\dots, M-1 \text{ and } q=0,1,\dots,n-1 \quad (1)$$

Each of these fourier transforms were then analysed. However, only absolute values were plotted for obtaining the amplitude spectrum. The data generated are given in the next section. Once these plots were obtained, then the peaks were analysed. Certain metrics were used for computing the nature of the plots. These metrics later served as the features that were used for the purpose of classification. The features that were extracted from these plots were the range, mean and the standard deviation of the frequency plots, using the following,

$$\mu = \frac{1}{n} \sum_{i=1}^n X_i \quad (2)$$

$$\sigma = \sqrt{\frac{1}{n} \sum_{i=1}^n (X_i - \mu)^2} \quad (3)$$

These features then served as an input towards the neural network, which was used for classifying the prints depending upon its source. The fundamental banding frequencies themselves can't be used as features, as they are unreliable. But aggregations of both the fundamental as well as the harmonic frequencies are to be analysed.

For classifying the samples, a multilayer peceptron based artificial neural network was used with a backpropagation training technique. There is a single hidden layer and the features are fed as the network input. The input and output layers are associated by this hidden layer. The number of output neurons is set according to the number of print classes. Each print sample is associated to the output neuron which exhibits highest activation level. As stated above, the ANN is trained by using a backpropagation training method, which aims towards reducing the mean square error between the targets and the output [25]. It is most essential to determine the correct number of neurons in the hidden layer, as the cost for computation depends on it.

The input contained of a 3x300 matrix, which meant that there were 300 samples and each had 3 features which were used. The targets also had a 3x300 matrix which depicted the classes to which the samples belonged. The samples were equally spaced as is evident from the number of samples selected. The number of neurons determines the processing cost, with lesser neurons, there is always a risk of false-classifications but with higher number of neurons there might be the problem of over-fitting. The numbers of neurons were determined empirically, the general thumb rule is,

$$X = \sqrt{M \times N} \quad (4)$$

where X is the number of neurons the hidden layer and M and N that in the input and output layers respectively. After each

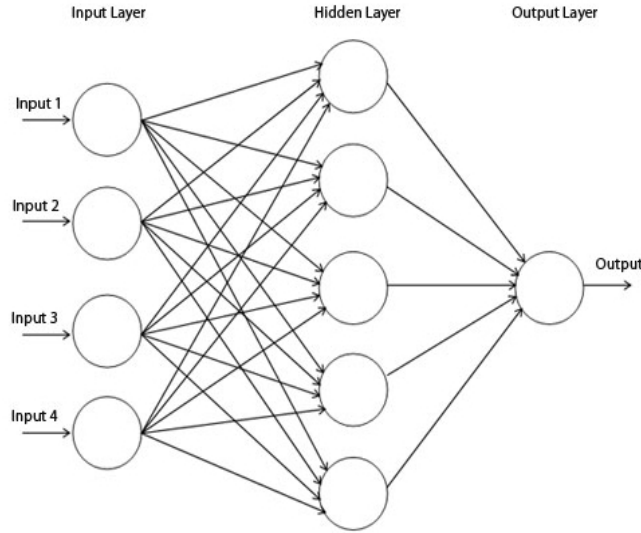


Figure 2: Architecture of a typical neural network

iteration, the connection weights are modified to minimize the error of reply [26]. This correction is made by:

$$\Delta W_{ji} = \eta \delta_j f'(a_i) \quad (5)$$

Where ΔW_{ji} the adjustment weight between neuron j and neuron i from previous layer; $f'(a_i)$ is the output of neuron i , η is the learning rate and δ_j depends on the layer.

$$\delta_j = (Y_j - \hat{Y}_j) f'_j(a_j) \quad (6)$$

the means square errors, in case of a supervised learning algorithm, let us consider the following,

$$\{p_1, t_1\}, \{p_2, t_2\}, \dots, \{p_n, t_n\} \quad (7)$$

where p_1 and t_q are the input and target provide to the network. The error after each input is the difference between the output to the target. It can be expressed as follows, where $t(k)$ is the target and

$\alpha(k)$ is the output from the network,

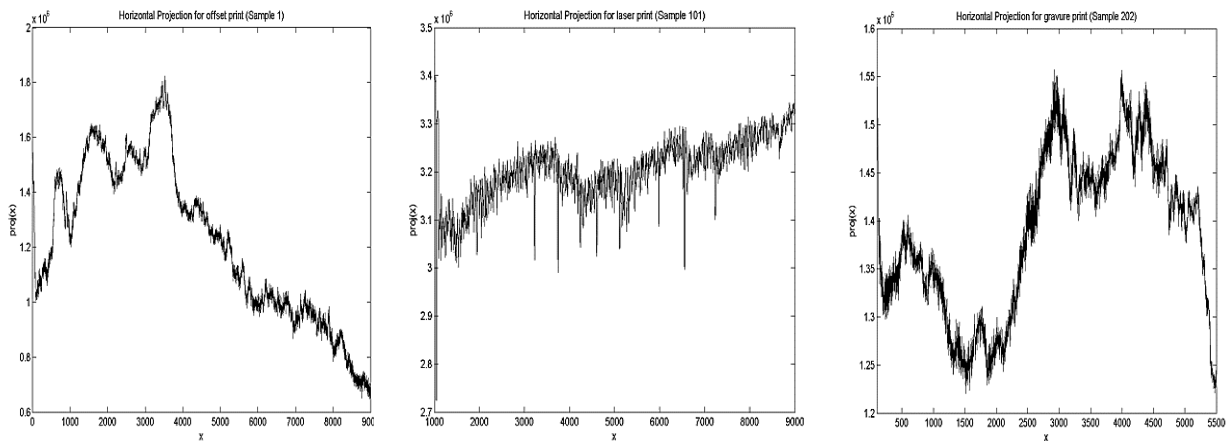


Figure 3: Horizontal Projections of images from three classes

Where Y_j is the expected value and \hat{Y}_j is the current output value of neuron j . The objective for realizing the performance of the network, the mean square error has to be reduced. As stated before, the standard performance of a perceptron lies in the fact of reducing

$$mse = \frac{1}{Q} \sum_{k=1}^Q e(k)^2 = \frac{1}{Q} \sum_{k=1}^Q (t(k) - \alpha(k))^2 \quad (8)$$

Experimental Data

The given methods were tested on a total of 300 images, where 100 images each were taken from offset, gravure and laser printers. The following represents, the data that were obtained after the processing stages. The first step involved, projecting the graylevel data horizontally. This was followed by a fourier analysis of the plot. And finally the features extracted from the plots were fed into the neural network for classification. The following plots are for three projection of offset, laser and gravure prints respectively.

can be visualised through the frequency plots as shown before.

Of the 300 samples taken from each of the classes, the features that were extracted were standard deviation, range and mean for the plots. The primary features that were chosen for the purpose of defining a curve and hence a class as such as mentioned before were standard deviation, range and mean. These three formed as the feature which represents each of the class and were fed into the network against each of the samples. The variations of the three features with every sample and that among each other are provided

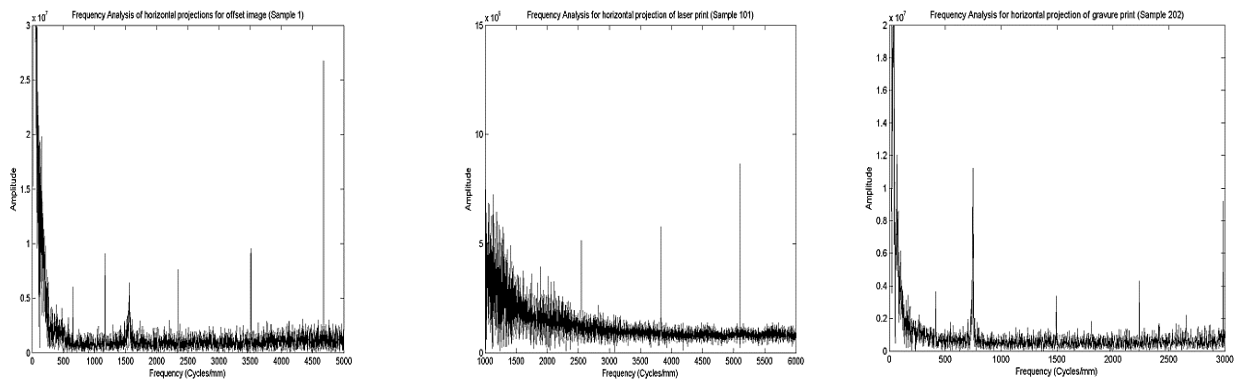


Figure 4: Frequency Analysis of the projections

The horizontal projections were further processed by means of use of a fourier transform and the results were analysed for feature extraction. The frequency plots are provided below.

Table 1: Fundamental banding frequency obtained after the fourier transform

	Offset (Sample 1)	Laser (Sample 101)	Gravure (Sample 202)
Fundamental Banding Frequency (Cycles/mm)	4750 and 3500 Cycles/mm	5100 Cycles/mm	750 Cycles/mm

The results for frequency analysis were noteworthy. As is evident from the frequency plots, there are definitive peaks that can be found from the plots. This indicates that there are banding frequencies which are present in those images. The presence of banding frequency may not be perceived by human visual system, but it can be clearly said that presence of embedded periodic noise

below and it defines how the various features have clear boundaries for each of the classes which have implications that these features can be used well for definitively identifying them when they are fed into the network. The neural network was trained using the remaining of the samples. Of the total 300 samples used, 210 samples were used for training and each of remaining 15% of the 30% were used for testing and validating the network. The neural network resulted in classification of the samples into the aforesaid three categories. In order to find the number of neurons in the hidden layer, empirical methods were used in this work. The number of neurons were incremented from 1 up to 10 by a factor of 1 and then up to 40 by 5. The performance of the network upon varying the number of neurons in the hidden layer is provided below. The rate of classification has increased with increment of number of neurons, but has stabilised after 10 neurons, which has also been depicted later. And the results were plotted both performance wise and the confusion matrix as has been provided below. The network performance was tested up to 200 iterations, with a 10 neuron hidden layer, by examining the MSE and the percentage of correct classifications in the training and test sets.

The results are given in Table 2.

Table 2: Confusion Plot for training sets with increasing number of neurons

Number of Neurons	Class	1	2	3	Total	Correct Classification
1	1	0	0	1	0.3	0
	2	0	99	1	100	0.99
	3	100	0	100	200	0.5
2	1	0	0	0	0	0
	2	9	98	1	108	0.93
	3	20	1	100	121	0.8264
3	1	85	21	2	108	0.787
	2	0	99	0	99	0.99
	3	10	70	43	123	0.349
4	1	88	2	7	97	0.907
	2	0	98	23	121	0.809
	3	1	0	100	100	1
5	1	100	20	0	120	0.833
	2	0	80	30	110	0.727
	3	0	0	100	100	1
6	1	63	34	79	176	0.358
	2	37	65	22	124	0.524
	3	0	0	100	100	1
7	1	100	0	0	100	1
	2	23	100	2	125	0.8
	3	5	45	98	148	0.662
8	1	100	23	66	89	1
	2	0	99	10	109	0.908
	3	0	0	100	100	1
9	1	93	0	5	98	0.949
	2	0	99	1	100	0.99
	3	47	0	98	145	0.676
10	1	100	0	0	100	1
	2	0	99	1	100	0.99
	3	0	0	100	100	1
15	1	102	0	0	102	1
	2	8	79	1	88	0.898
	3	90	20	100	210	0.47
20	1	100	0	0	100	1
	2	0	99	1	100	0.99
	3	0	0	100	100	1
25	1	100	21	2	123	0.813
	2	0	100	0	100	1
	3	0	8	99	107	0.9252
30	1	100	0	6	106	0.943
	2	2	99	0	101	0.98
	3	7	0	101	108	0.9352
35	1	100	0	0	100	1
	2	0	99	0	99	1
	3	0	0	100	100	1
40	1	100	0	0	100	1
	2	1	99	0	100	0.99
	3	0	0	100	100	1

It was observed that the percentage of classification increased rapidly with the increment of initial number of neurons, but it became almost negligible after 10 neurons, the percentage decreased to some extent beyond 30 neurons. Also the mean square errors decreased with increased number of iterations rapidly at the initial level, but remained unchanged with a further increase of iteration count, at this point the values almost became stable. The rate of classification increased rapidly up to 140 iterations for the training set and testing set, but beyond that the testing set became almost

stationery. As is evident from the mean and standard deviation of the correct classifications obtained from the network, the rate of classification has been quite high. The performance of the classifier is provided in the table, which summarises how well the images were classified to the class of their origin. The network outputs were noted and the network was tested against multiple test samples from the real world and the results were quite satisfactory. As given above the rate of classification was sufficiently high for the samples provided which is evident from the performance of the network after final training stages. The overall performance of the network was $96.3 \pm 2\%$.

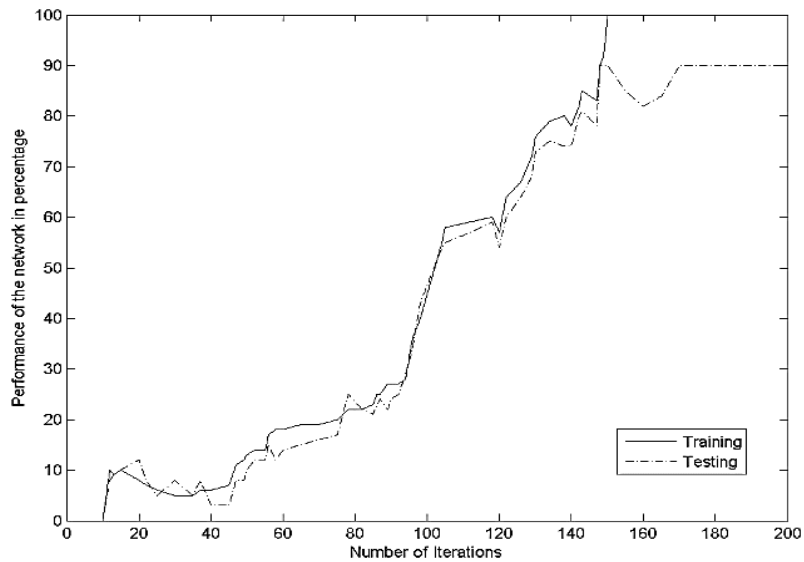


Figure 5: Performance of the network with respect to the number of iterations

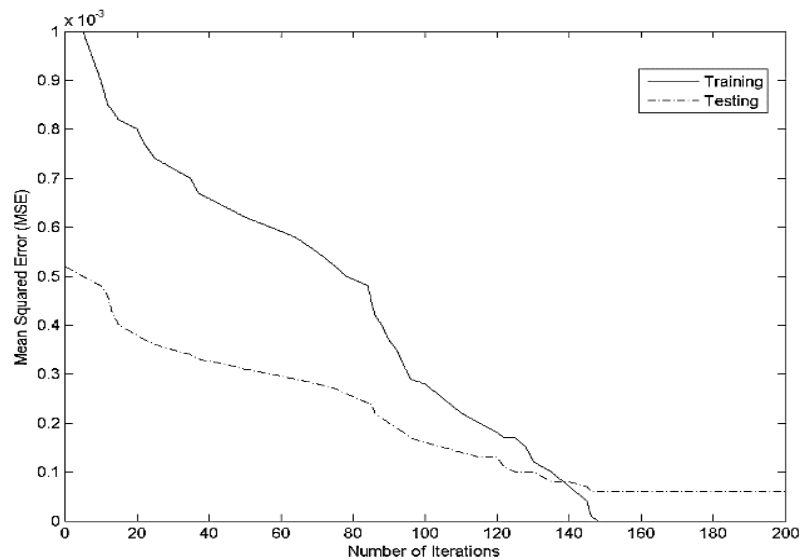


Figure 6: Mean squared error with respect to the number of iterations

Table 3: Mean and Standard Deviation values for correctly classified sets

	1	2	3
Mean	0.9537	0.9475	0.9873
Std	0.0685	0.0694	0.0283

Conclusions

This study provides a newer outlook to a problem, which itself is difficult to solve for. The presence of banding is a common phenomenon in most EP based printers. Much has been studied with respect to its properties, and its detection. The problem of reducing its visibility to the human perception by thresholding techniques has been suggested in [22]. However the real challenge for this study was to find whether these intrinsic properties are present in the offset or gravure prints at all and can be used for identifying them. The banding frequencies for offset and gravure prints are not as predominantly visible as those of the EP prints, but as our study shows, that a frequency analysis of these prints clearly depicts the presence of embedded banding signal or noise in all those prints. There are a large number of government documents which are printed in offset or gravure methods, this can be a way for usefully identifying the source of any printed image, which has wide applications in duplicate or forged document identification and tracking. The features that were extracted from the images and they served has distinguishing parameters defining a particular print. The different print classes viz., offset, laser and gravure were formed depending on the values of the features. A neural network was then trained to learn the classes as defined by their features. Increasing the number of neurons led to enhanced classification rate until an asymptote was reached, after which over fitting occur, this should be avoided in order to save computation time. The results from the neural network provided a distinct classification between the classes and it was observed from the performance of the network that it is indeed possible to differentiate and identify these classes as they exist by the methods described in this paper. The network was tested with real life data and the results were encouraging. Further work would include increased number of features including texture analysis and wavelet decompositions of the images to enhance the classification rates.

References

[1] EJ Delp . Is your document safe: an overview of document and print security. In: Proceedings of the IS&T International Conference on Non-Impact Printing, San Diego, CA; September 2002.

[2] P-J Chiang , AK Mikkilineni, Arslan O, Kumontoy RM, Chiu GT-C, Delp EJ, et al. Extrinsic signature embedding in text document using exposure modulation for information hiding and secure printing in electrophotography. In: Proceedings of the IS&T's NIP21: International Conference on Digital Printing Technologies, vol. 21. Baltimore, MD; October 2005. p. 231-4.

[3] Khanna, N., Mikkilineni, A. K., Martone, A. F., Ali, G. N., Chiu, G. T. C., Allebach, J. P., & Delp, E. J. (2006). A survey of forensic characterization methods for physical devices. *digital investigation*, 3, 17-28.

[4] Ali GN, Chiang P-J, Mikkilineni AK, Allebach JP, Chiu GT-C, Delp EJ. Intrinsic and extrinsic signatures for information hiding and secure printing with electrophotographic devices. In: Proceedings of the

IS&T's NIP19: International Conference on Digital Printing Technologies, vol. 19. New Orleans, LA; September 2003. p. 511-5.

[5] Ali GN, Chiang P-J, Mikkilineni AK, Chiu GT-C, Delp EJ, Allebach JP. Application of principal components analysis and Gaussian mixture models to printer identification. In: Proceedings of the IS&T's NIP20: International Conference on Digital Printing Technologies, vol. 20. Salt Lake City, UT; October/November 2004. p. 301-5.

[6] Mikkilineni AK, Chiang P-J, Ali GN, Chiu GT-C, Allebach JP, Delp EJ. Printer identification based on textural features. In: Proceedings of the IS&T's NIP20: International Conference on Digital Printing Technologies, vol. 20. Salt Lake City, UT; October/November 2004. p. 306-11.

[7] Mikkilineni AK, Chiang P-J, Ali GN, Chiu GT-C, Allebach JP, Delp EJ. Printer identification based on graylevel co-occurrence features for security and forensic applications. In: Proceedings of the SPIE International Conference on Security, Steganography, and Watermarking of Multimedia Contents VII, vol. 5681. San Jose, CA; March 2005. p. 430-40.

[8] Mikkilineni AK, Arslan O, Chiang P-J, Kumontoy RM, Allebach JP, Chiu GT-C, et al. Printer forensics using svm techniques. In: Proceedings of the IS&T's NIP21: International Conference on Digital Printing Technologies, vol. 21. Baltimore, MD; October 2005. p. 223-6.

[9] Arslan O, Kumontoy RM, Chiang P-J, Mikkilineni AK, Allebach JP, Chiu GT-C, et al. Identification of inkjet printers for forensic applications. In: Proceedings of the IS&T's NIP21: International Conference on Digital Printing Technologies, vol. 21. Baltimore, MD; October 2005. p. 235-8.

[10] Mikkilineni AK, Chiang P-J, Suh S, Chiu GT-C, Allebach JP, Delp EJ. Information embedding and extraction for electrophotographic printing processes. In: Proceedings of the SPIE International Conference on Security, Steganography, and Watermarking of Multimedia Contents VIII, vol. 6072. San Jose, CA; January 2006. p. 385-96.

[11] Mikkilineni AK, Ali GN, Chiang P-J, Chiu GT-C, Allebach JP, Delp EJ. Signature-embedding in printed documents for security and forensic applications. In: Proceedings of the SPIE International Conference on Security, Steganography, and Watermarking of Multimedia Contents VI, vol. 5306. San Jose, CA; January 2004. p. 455-66.

[12] Mace, John. Printer Identification Techniques and Their Privacy Implications. University of Newcastle upon Tyne, Computing Science, 2010.

[13] Rawashdeh NA, Shin I, Donohue KD, and Love S, Printer Banding Estimation Using the Generalized Spectrum, In: Proceedings of SPIE, volume 6059, Image Quality and System Performance III, SPIE, Bellingham, WA, 2006.

[14] Kane PJ, Bouk TF, Burns PD, and Thompson AD, Quantification of Banding, Streaking and Grain in Flat Field Images, In: Image Processing, Image Quality, Image Capture, Systems Conference, Society for Imaging Science and Technology, 2000, p. 79-83.

[15] Jang W and Allebach JP, Simulation of Print Quality Defects, In: International Conference on Digital Printing Technologies, 2002, p. 543-548.

[16] Ewe MTS, Chiu GTC, Grice J, Allebach JP, Foote W and Chan CS, Banding Reduction in Electrophotographic Processes Using a Piezoelectric Actuated Laser Beam Deflection Device, In: Journal of Imaging Science and Tech., vol. 46, no. 5, 2002, p. 433-442.

[17] You J-H, Kim H-C, and Han S-Y, Banding Reduction in Electrophotographic Printer, In: International Conference on Digital Printing Tech., 2004, p. 470-473.

[18] Briggs JC, Murphy M, and Pan Y, Banding Characterization for Inkjet Printing, In: Image Processing, Image Quality, Image Capture, Sys. Conference, Society for Imaging Science and Technology, 2000, p. 84-88.

- [19] Chen MC, Chiu GT-C, and Allebach JP, Characterization of Chromatic Banding Artifact for Secondary Colors in a Polychrome Electrophotographic Process, In: International Conference on Digital Printing Technologies, 2004, p. 464-469.
- [20] Campbell FW and Robson JG, Application of Fourier Analysis to the Visibility of Gratings, *Journal of Physiology*, vol. 197, 1968, p. 551-566.
- [21] Cui C, Cao D, and Love S, Measuring Visual Threshold of Inkjet Banding, In: Image Processing, Image Quality, Image Capture, Systems Conference, Society for Imaging Science and Technology, 2001, p. 84-89.
- [22] Wu W, Dalal EN, and Rasmussen RD, Perceptibility of Non-sinusoidal Bands, In: International Conference on Digital Printing Tech., 2002, p. 462-466.
- [23] Bang Y, Pizlo Z, and Allebach JP, Discrimination Based Banding Assessment, International Conference on Digital Printing Technologies, 2003, p. 745-750.
- [24] Lin G-Y, Grice JM, Allebach JP, Chiu GT-C, Bradburn W, Weaver J. Banding artifact reduction in electrophotographic printers by using pulse width modulation. *Journal of Imaging Science and Technology* July/August 2002;46, no. 4:326-37.
- [25] R. Hecht-Nielsen, *Neurocomputing*, Addison-Wesley, 1990.
- [26] Reby, D., Lek, S., Dimopoulos, I., Joachim, J., Lauga, J., & Aulagnier, S. (1997). Artificial neural networks as a classification method in the behavioural sciences. *Behavioural processes*, 40(1), 35-43.

Author Biography

Shankhya Debnath and Jitamitra Bagchi are currently final year engineering students pursuing their Bachelors in Engineering in Printing Engineering from the Department of Printing Engineering, Jadavpur University, Kolkata, India.